Neuroendocrinology

Programmed cell death ligands expression drives immune tolerogenesis across the diverse subtypes of neuroendocrine tumours.

Pinato D.J. Vallipuram A. Evans J.S. Wong C. Zhang H. Brown M. Dina R.E. Trivedi P. Akarca A.U. Marafioti T. Mauri F.A. Sharma R.

Neuroendocrinology

Manuscript:	NEN-2019-11-27/R2 RESUBMISSION
Title:	Programmed cell death ligands expression drives immune tolerogenesis across the diverse subtypes of neuroendocrine tumours.
Authors(s):	David James Pinato (Corresponding Author), Anu Vallipuram (Co-author), Joanne S Evans (Co-author), Clement Wong (Co-author), Hua Zhang (Co-author), Matthew Brown (Co-author), Roberto E Dina (Co-author), Pritesh Trivedi (Co-author), Ayse U Akarca (Co-author), Teresa Marafioti (Co-author), Francesco A Mauri (Co-author), Rohini Sharma (Co-author)
Keywords:	Biomarkers, Gastroenteropancreatic neuroendocrine tumors, Immunohistochemistry, Immunotherapy, Neuroendocrine tumors, Pancreatic neuroendocrine tumors, Treatment
Type:	Research Article

Programmed cell death ligands expression drives immune tolerogenesis across the diverse subtypes of neuroendocrine tumours.

David J. Pinato[1], Anu Vallipuram[1], Joanne S. Evans[1], Clement Wong[1], Hua Zhang[2], Matthew Brown[1], Roberto E. Dina[3], Pritesh Trivedi[3], Ayse U Akarca[4], Teresa Marafioti[4], Francesco A. Mauri[3], Rohini Sharma[1].

1.   Department of Surgery & Cancer, Imperial College London, Hammersmith Hospital, Du Cane Road, W120HS London, UK.

2.   Dana-Farber Cancer Institute, Department of Medical Oncology, LC-4112, 450 Brookline Avenue, 02215 Boston, MA, USA.

3.   Department of Histopathology, Imperial College London, Hammersmith Hospital, Du Cane Road, W120HS London, UK.

4.   Department of Histopathology, University College London Hospital, Rockefeller Building, University Street, WC1E6JJ London, UK.

To whom correspondence should be addressed:

Dr David J. Pinato, MD MRes MRCP PhD
NIHR Academic Clinical Lecturer in Medical Oncology
Imperial College London Hammersmith Campus,
Du Cane Road, W12 0HS, London (UK)
Tel: +44 0207 594 2799 E-mail: david.pinato@imperial.ac.uk

Abstract.

Introduction: A comprehensive characterisation of the tumour microenvironment is lacking in neuroendocrine tumours (NETs), where programmed cell death-1 receptor-ligand (PD-1/PD-L1) inhibitors are undergoing efficacy testing.

Objective: We investigated drivers of cancer-related immunosuppression across NETs of various sites and grade using multi-parameter immunohistochemistry and targeted transcriptomic profiling.

Methods: Tissue microarrays (n=102) were stained for PD-L1 & 2, Indoleamine-deoxygenase-1 (IDO-1) and evaluated in relationship to functional characteristics of tumor-infiltrating T-lymphocytes (TILs) and biomarkers of hypoxia/angiogenesis. PD-L1 expression was tested in circulating tumour cell (CTCs, n=12) to evaluate its relationship with metastatic dissemination.

Results: PD-L1 expression was highest in lung NETs (n=30, p=0.007), whereas PD-L2 was highest in pNETs (n=53, p<0.001) with no correlation with grade or hypoxia/angiogenesis. PD-L1$^+$ NETs (n=26, 25%) had greater CD4$^+$/FOXP3$^+$ and CD8$^+$/PD1$^+$ TILs (p<0.001) and necrosis (p=0.02). CD4$^+$/FOXP3$^+$ infiltrate was highest PD-L1/IDO-1 co-expressing tumours (p=0.006). Grade 3 well-differentiated NETs had lower CD4$^+$/FOXP3$^+$ and CD8$^+$/PD1$^+$ TILs density (p<0.001) and Nanostring immune-profiling revealed enrichment of macrophage-related transcripts in cases with poorer prognosis. We identified PD-L1(+) CTC subpopulations in 75% of evaluated patients (n=12).

Conclusions: PD-L1 expression correlates with T-cell exhaustion independent of

2

tumour hypoxia and is enhanced in a subpopulation of CTCs, suggesting its relevance to the progression of NETs. These findings support a potential therapeutic role for PD-L1 inhibitors in a subset of NETs.

Accepted manuscript

3

Introduction.

The natural history of neuroendocrine tumours (NETs) is heterogeneous, encompassing disease variants with highly aggressive as well as remarkably indolent clinical course[1]. Accumulating evidence suggests that NETs rely heavily on the Programmed-cell Death-1 (PD-1) axis to circumvent immune rejection, implying that PD-ligand 1 (PD-L1)-overexpressing NETs may be potentially sensitive to PD-1/PD-L1-targeting immune checkpoint inhibitors (ICPI)[2-4], as demonstrated in other indications. The tumoricidal effect of ICPIs strongly depends on the reconstitution and clonal expansion of cytotoxic CD8^{+} T-cell function. However, most studies that postulate NETs as potentially sensitive to ICPI focused on cases of either gastrointestinal[5, 6] or thoracic origin, evaluated uniquely for PD-1/PD-L1 expression[7]. Tumour-mediated CD8^{+} T-cell dysfunction is a multi-faceted process and can be fostered by a number of factors including tumour hypoxia, a key hallmark of progression in NETs[8], and by concurrent activation of metabolic drivers such as Indoleamine 2,3 dioxygenase-1 (IDO-1), which promotes regulatory T-cell (T-reg) differentiation[9] and reduces CD8^{+} effector activity via tryptophan depletion. The relative functional contribution of each of these key mechanisms of immune suppression has not been fully understood in NETs. This is a point of consequence in a phase of rampant expansion of immunotherapy, where IDO-1 inhibitors and anti-angiogenics are being prospectively tested in combination with ICPIs[10].

To address these limitations, we designed this study to provide a comprehensive functional characterization of the anti-cancer immune response in a well-annotated series of tissue specimens using multi-parameter immunohistochemistry and targeted

4

transcriptomics. In addition, as a secondary aim, we set out to establish the prevalence and clinico-pathologic role of PD-L1 expression in circulating tumour cells (CTCs), a biomarker of aggressive behavior that is emerging as a promising alternative to tissue-based diagnostics in NETs[11].

Materials and Methods.

Tissue Samples.

Tissue microarrays (TMA) were constructed from a patient series including 102 consecutive patients undergoing surgical resection for NETs at Imperial College NHS Trust from 1988 to 2017(15). This case series forms part of a previously published study[12]. Grading of NETs followed the World Health Organisation 2010 guidelines. Recognizing the heterogeneity of high-grade NETs, tumors that were defined as high grade clustered within the well-differentiated Grade 3 NETs (G3-WDNETs) category[13]. The study was approved by the Imperial College Tissue Bank (Ref. R14066-2A) and conducted in accordance to the principles of the Declaration of Helsinki.

Immunohistochemistry.

We performed single marker immunostaining for PD-L1 (E1L3N; Cell Signaling Technology, Danvers, Massachusetts, USA), PD-L2 (3500395, Sigma Aldrich, St. Louis, Missouri, USA), IDO-1 (D5J4E; Cell Signaling Technology), VEGF-A (Santa Cruz Biotechnology, Santa Cruz, California, USA), Hif-1α (AbCam, Cambridge, UK) and Ki-67 (Leica Microsystems, Wetzlar, Germany) on a Leica Bond RX stainer (Leica, Buffalo,

5

Illinois, USA) on 5-micron TMA slides (**Supplementary Methods**). To evaluate the phenotypic characteristics of tumour-infiltrating lymphocytes one 2-micron TMA slide underwent multi-colour immune cell phenotyping for PD-1 (clone NAT 105/E3), CD4 (Spring Biosciences, clone SP35), CD8 (clone SP239) and FOXP3 (clone 346/E7) based on a previously optimised protocol at University College London[14]. Expression of the candidate biomarkers was evaluated using the histoscore method (range 0-300) as described before[12]. For multiplex IHC, we analysed number of immuno-positive cells/mm^2 of tissue following review of specificity of staining by a consultant histopathologist with expertise in evaluating multi-colour IHC (T.M.).

Hypoxic chamber experiment.

Pancreatic NET cell lines QGP-1 and BON-1 were purchased from the American Type Culture Collection (Manassas, Virginia, USA). SKBR3 and MBA-MD-231 were used as control cell lines (**Supplementary Materials**). Cells were incubated in hypoxic conditions using the Whitley H35 hypoxystation (Don Whitley, Shipley, West Yorkshire, UK) in standard media in an atmosphere of 1% O_2, 94% N_2 and 5% CO_2 for 24 hours and lysed in parallel with normoxic controls. Protein expression was evaluated by immunoblotting (**Supplementary Methods**).

CTC enumeration and PD-L1 staining.

A total of 7.5 ml of EDTA-anticoagulated blood was used for CTC detection using the FDA-approved CellSearch system (Janssen, Beerse, Belgium). Blood samples were processed within 72 h from venipuncture using the CellSearch CXC kit (Janssen). With this method, CTCs are enumerated by visual detection of a subpopulation of EpCAM(+),

6

Cytokeratin(+), DAPI(+), CD45(-) intact cells. Using pre-published methodology, we used the anti-human-PD-L1 phycoerythrin conjugate antibody (Cat. FAB1561P R&D Systems Minneapolis, USA) at the final concentration of 20 µg/ml to allow for phenotypic characterization of CTC using the 4th channel of the CellSearch system[15].

NanoString Immune profiling.

We performed H&E-guided manual microdissection of target tumour tissue in a subset of 12 samples and extracted total RNA on four 10 µM-thick tissue sections using the Qiagen RNAeasy FFPE kit (Qiagen, Venlo, NL, Cat Nr. 73504) according to the manufacturer's instructions. We performed targeted transcriptomic profiling using the NanoString PanCancer Immune panel on an nCounter® Analysis System (NanoString Technologies, Seattle, USA, **Supplementary Methods**). Samples flagged for high normalisation values or with quality control standards falling outside default settings were examined carefully and a total of 2 samples were excluded, leaving 10 for final analysis.

Statistical Analysis.

Pearson's Chi square or Fisher's exact tests were used to elucidate any significant associations between categorical variables as appropriate. Associations were considered statistically significant when the resulting p value was < 0.05. Analysis was performed using SPSS software version 11.5 (SPSS inc., Chicago, IL, USA) and GraphPad PRISM (GraphPad software inc., La Jolla, CA, USA). Differential expression of genes of interest was determined using the false discovery rate method (FDR) of Benjamini and Hochberg, with pre-defined q-value of 5%

Results.

Patients, Tumour Characteristics and Survival.

The clinico-pathological features reconstructed from the 102 patients included in the study are summarized in (**Table 1**). The median OS of the whole cohort was 10.1 years (95% CI 9.2-10.9), with 19 (19%) patients having died at the time of analysis. Uni-variable analyses of survival confirmed tumour grade (median OS 3.2 years for G3 versus not reached for G1-2, HR 7.3 95%CI 2.7-19.6 years, p<0.001) and necrosis (median OS 7.4 years versus not reached, HR 6.4 95%CI 2.3-18.1, p<0.001) as predictors of worse OS.

Expression of immune-related biomarkers in NETs.

Overall, 26 patients (25%) had evidence of intra-tumoural PD-L1 expression with a mean IHS of 8.6 (median 0, range 0-270). Tumour cell expression of PD-L2 was found in 41 specimens (40%): mean IHS was 60 (median 45, range 0-270**)**.

IDO-1 expression was detected in 42 patients (40%), 24 of pancreatic, 5 of gastrointestinal and 13 of extra-gastrointestinal origin (p=0.51). Mean IDO IHS was 46 (median 0, range 0-300, **Figure 1A-C**).

PD-L1, PD-L2 and IDO-1 expression was not influenced by grade (p=0.67, p=0.13, p=0.73) or stage (p=0.24, p=0.51, p=0.15). PD-ligands expression varied significantly according to primary site, with PD-L1 immunopositivity being highest in lung NETs (Chi-

8

square 5.40, d.f.=2, p=0.007) and PD-L2 expression being highest in pancreatic NETs (Chi-square 26.4, d.f.=2, p<0.0001, **Figure 1D-E**). The presence of tumour necrosis was associated with higher levels of tumoural PD-L1 expression (Mann Whitney p=0.03) and lower PD-L2 expression (p=0.02), whereas vascular invasion inversely correlated with PD-L2 expression (p=0.003, **Figure 1F-G**).

PD-ligands expression influences the tumour microenvironment in NETs.

We used multiplex-IHC to investigate the relationship between PD-ligands and cytotoxic T-cell exhaustion (CD8$^+$/PD1$^+$) and regulatory T-cell (T-reg) function (CD4$^+$/FoxP3$^+$). As shown in **Figure 2A-D**, the microenvironment of PD-L1$^+$ NETs was significantly enriched in T-reg and immune-exhausted CD8$^+$/PD1$^+$ T-cells. Tumour specimens of higher grade were characterized by lower density of CD8$^+$/PD1$^+$ and CD4$^+$/FoxP3$^+$ infiltrate (**Figure 2E**). We found PD-L1/IDO-1 co-immunoexpression in 13% of NETs (Chi-square 4.34, d.f.=1, p=0.03), with PD-L1$^+$/IDO-1$^+$ tumours being characterized by denser CD4$^+$ infiltrates and higher proportion of infiltrating T-regs (Kurskal-Wallis p=0.006, **Figure 2F-G**).

Whilst neither PD-L1 (Log-rank p=0.85) nor PD-L2 expression (p=0.95) or IDO-1 expression (p=0.77) independently predicted for OS (**Supplementary Figure 1**), we found that patients displaying evidence of necrosis, a predictor of adverse prognosis in our patient cohort, had significantly higher levels of CD8$^+$/PD1$^+$ and CD4$^+$/FoxP3$^+$ infiltrating cells (p<0.001, **Figure 2H**).

The relationship between PD-L1 expression and hypoxia in pNETs.

9

We evaluated the relationship between PD ligands expression and a selected panel of biomarkers reflective of the hypoxic/angiogenic response in a subset of patients with pNETs (n=47) in view of its documented pathogenic and prognostic role in this subset of tumours (**Supplementary Figure 2**). We found no difference in the expression of VEF-A, Hif-1α and CaIX in relationship to the expression of PD-L1 or PD-L2.

After evaluating baseline PD-L1 and PD-L2 expression in immortalized NET cells (**Figure 2I**), we utilized an *in vitro* model of tumour hypoxia to demonstrate that none of the assayed cell lines displayed evidence of PD-L1 over-expression following 24h-incubation in 1% O_2, suggesting independence between hypoxia and tumour-cell expression of PD-L1 (**Figure 2L**).

Transcriptomic analysis.

To complement our multiplex-immunohistochemistry data showing depletion of CD8/PD1 and CD4/FoxP3 cells in high-grade NETs we performed an exploratory targeted transcriptomic analysis of a limited subset of 10 patient samples using NanoString technology (**Supplementary Figure 3, Table S1**) to provide mechanistic insight into the molecular drivers characterising the tumour immune microenvironment in this poor prognostic subgroup. As shown in **Fig 3A** we report repression of transcripts involved in leukocyte function and complement and up-regulation of cytotoxicity-related genes in gastrointestinal (GI) compared to extra-GI (eGI) NETs. Similarly, we report significant up-regulation of interleukins and repression of adhesion-related genes in patients with poorer prognosis, with significant down-regulation of the B-cell lymphotropic cytokine CXCL13 alongside other genes reflective of tumour associated

10

macrophage biology (CD68, CSF1R) and T cell activation (CD4, CD84, PI3KCG, TNFRSF11A) (**Fig.3B**).

Expression of PD-L1 in CTCs.

Peripheral blood samples from a total of 12 consecutive, unselected patients with advanced NETs were processed for CTC quantification using the CellSearch system (**Table 2**). In patients with CTC$\geq$1 (n=10, 83%), the median CTC count was 3 (range 1-6). In total 9 patients out of 12 (75%) showed a subpopulation of CTCs expressing PD-L1 (**Fig.4A**) In patients with CTC$\geq$1 the median percentage of PD-L1$^+$ CTCs was 79% (range 0-100, **Fig.4B**). Patients whose PD-L1$^+$ CTC count was $\geq$3 (i.e. above the median) had a higher frequency of extra-hepatic spread to other visceral organs including lung, bones and peritoneal cavity (1/10 versus 2/2 patients, Fisher Exact Test p=0.04).

Discussion.

Clinical responses to ICPI are limited to a fraction of patients across indications, a finding that has instigated the discovery of novel actionable drivers of cancer-related immune-suppression that can be selectively targeted to enhance anti-tumour immune reconstitution[16]. Avoidance of T-cell-mediated cytolysis by progressive malignancy is sustained by parallel up-regulation of alternative immune-modulatory signals within the tumour microenvironment including PD-L2 or IDO-1[17], which have been shown to promote clinical resistance to PD-1/PD-L1 checkpoint inhibitors. In addition, sustained

11

neo-angiogenesis, primarily through VEGF signaling, exerts multi-faceted immune-suppressive effects by preventing CD4^{+} and CD8^{+} T-cell maturation, promoting regulatory T-cell (T-Reg) differentiation and inducing exhaustion of effector T-cell responses by up-regulation of PD-1 and its ligands[18].

In this study, we found significant heterogeneity in PD-ligands expression across various NET subtypes, with PD-L1 being more prevalent in lung and PD-L2 in pNETs, suggesting contextual differences in the expression of key molecular drivers of cancer immunosuppression. Our study mirrors previously published evidence demonstrating low expression levels of PD-L1 in pancreatic and intestinal NETs and cytoplasmic PD-L2 expression in a significant proportion of these tumors, independent of underlying mutational status[19]. Site-specific heterogeneity in PD-L1 expression has also been described in NETs, with duodenal tumors having shown evidence of stronger PD-L1 expression over jejunal/ileal NETs, whereas little comparative evidence exists with regards to lung NETs[6].   In our study, PD-L1 expression strongly correlated with CD4^{+}/FOXP3^{+} and CD8^{+}/PD1^{+} TIL density, suggesting polarization of intra-tumoural T-cells to a type-1 response. PD-L1^{+}/TIL^{+} or type-1 tumours, are thought to be sensitive to single-agent PD-1/PD-L1-targeted checkpoint blockade, due to the presence of an immune-reactive microenvironment where TILs are chemo-attracted to malignant cells but turned off by PD-L1 engagement[20]. Whilst the majority of analysed samples fitted this immunophenotype, G3WD tumours, a subgroup of NETs with poor prognosis and limited treatment options, displayed evidence of a less intense CD4^{+}/FOXP3^{+} and CD8^{+}/PD1^{+} infiltrate compared to low-grade NETs despite comparable PD-ligands expression levels, a finding that prompted us to explore alternative immune-biologic

12

mechanisms underlying the progression of this subset of tumours. In a pilot experiment using nanostring transcriptomic profiling of high-grade NETs, we confirmed enrichment of transcripts reflective of macrophage activation in patients characterized by worse survival outcomes, suggesting an important regulatory dynamic with T-cells that should be explored in future studies[21]. A recent study by Ferrata et al. is in support of our findings, having shown the tumour microenvironment of highly proliferating G3 NETs to be characterized by higher CD68 over CD8 infiltration, suggesting a more predominant role for myeloid-derived immune suppression in these tumours[4].

Interestingly, 13% of our patients displayed evidence of PD-L1/IDO-1 co-immunoexpression, which correlated with a denser T-regulatory infiltrate, suggesting that a tryptophan-depleted tumour microenvironment might exert synergistic effects with PD-ligands expression in promoting cancer immune-suppression[17]. IDO-1 shares with PD-L1 a strongly inflammation-driven transcriptional dependence, secondary in particular to interferon gamma signaling [22, 23]. IDO-1-mediated tryptophan catabolism is a mechanism of induction of T-regs from naïve T-cells[24] and tumours exhibiting higher levels of PD-1/PD-L1 and IDO-1/HLA-DR are exquisitely sensitive to anti-PD-1/PD-L1 checkpoint inhibition, suggesting a potential synergistic role from combined pathway inhibition[25]. However, recent failures in the development of combined IDO-1/PD-1 blockade in randomized controlled studies highlight the unexpected complexities in the modulation of kynurenine to tryptophan ratios within the tumour microenvironment as a strategy to reverse immune tolerance[26], a point that should be considered in the development of immunotherapy for NETs. The richness of other tryptophan-degrading enzymes such as tryptophan 2,3 dehydrogenase (TDO) or the dysregulation of Aryl

13

hydrocarbon receptors, the amino acid sensing signal transduction pathway that modulates immune-suppressive gene expression programs upon kynurenine ligation, have been advocated as mechanisms of resistance and treatment failure[27].

In our study, despite their association with an immune-suppressive microenvironment and tumour necrosis, a strongly adverse prognostic factor in NETs, PD-ligands and IDO-1 expression were not directly predictive of patients' survival. Prevalence and clinico-pathologic value of PD-L1 expression has been investigated mostly in gastro-entero-pancreatic tumours and reported to be highly variable across studies, ranging from <10%[5] to >50%[3]. The lack of a significant correlation between PD-L1 status and patients' survival mirrors published evidence, where the postulated role for PD-L1 expression as a predictor of survival[3] has not found confirmation in larger studies[6, 28, 29]. A number of factors might explain the high level of heterogeneity observed across studies, including inherent differences in patient selection, the influence of anti-tumour therapy on patients' survival and the extended survival times of early-stage patient cohorts. Nevertheless, the lack of association with survival does not limit the role of the tested biomarkers as putative predictors of benefit from ICPI.

Unlike other neuroendocrine malignancies[30], our data suggests PD-L1 expression to be independent from that of Hif-1α and its downstream targets VEGF-A and CaIX, key drivers of the hypoxic/angiogenic response and therapeutic targets of established efficacy in pNETs[31]. This finding, which we corroborated mechanistically *in vitro* using immortalized cell lines, denotes that hypoxia and PD-L1-mediated T-cell exhaustion might be independent drivers of pNETs progression.

14

In an attempt to further dissect the immunobiology of NETs we postulated whether PD-L1 expression might be involved in the process of metastatic dissemination of these tumours. Because CTCs are a prognostic biomarker linked to the metastatic potential of NETs[32], we elected to evaluate PD-L1 expression status in CTCs from a pilot study of 12 prospectively recruited patients with advanced disease. Interestingly, we found that the vast majority of patients harbored a population of PD-L1 positive CTCs and that higher CTC counts correlated with heavier metastatic burden. Whilst limited by small sample size, our results are provocative in suggesting that PD-L1 up-regulation in CTCs might facilitate the survival of metastasizing cells in the bloodstream through suppression of antitumor immune clearance[33]. This appears particularly relevant in NETs, where the activation of the PD-1/PD-L1 pathway in peripheral blood mono-nuclear cells is significantly associated with metastatic dissemination and disease evolution[5]. Furthermore, the isolation of PD-L1(+) CTCs, recently replicated in an increasing number of malignancies[15], ascribes metastatic NETs to the series of tumours where phenotypic characterization of CTCs might stand as a potentially useful surrogate of PD-L1 assessment in tumor specimens[34]. Larger studies exploring the relationship between PD-L1(+) CTC counts, matched diagnostic tumor specimens and response to anti-PD-1/PD-L1 therapies should be conducted to explore the clinical utility of this approach.

Our study acknowledges a number of limitations. Firstly, none of the patients included in our study were treated with immunotherapy, highlighting the need for the features of the tumour microenvironment described here to be validated in relationship to response and survival following ICPI. Secondly, whilst tissue microarrays are a validated technology in

15

the study of tissue biomarkers from archival material[28], their use could have led us to underestimate the broader heterogeneity in biomarker expression that can be better appraised by staining whole tumor sections.

To conclude, whilst clinical trials are underway to evaluate the efficacy of immunotherapy in NETs, our data suggest differential regulation of immune-tolerogenic pathways in the progression of these tumours and confirm the existence of a proportion of NETs showing immunobiologic features consistent with enhanced responsiveness to anti-PD-1/PD-L1 therapies. Consideration should be given to the quantification of these biomarkers in prospective studies as a measure to optimize the clinical development of anti-cancer immunotherapy.

Statements

Statement of Ethics. The study was approved by the Imperial College Tissue Bank (Ref. R14066-2A).

References.

1   Yao JC, Hassan M, Phan A, Dagohoy C, Leary C, Mares JE, Abdalla EK, Fleming JB, Vauthey JN, Rashid A, Evans DB: One hundred years after "carcinoid": Epidemiology of and prognostic factors for neuroendocrine tumors in 35,825 cases in the united states. J Clin Oncol 2008;26:3063-3072.

2   Roberts JA, Gonzalez RS, Das S, Berlin J, Shi C: Expression of pd-1 and pd-l1 in

17

poorly differentiated neuroendocrine carcinomas of the digestive system: A potential target for anti-pd-1/pd-l1 therapy. Hum Pathol 2017;70:49-54.

3   Wang C, Yu J, Fan Y, Ma K, Ning J, Hu Y, Niu W, Dong X, Wu Y, Li E, Dong D: The clinical significance of pd-l1/pd-1 expression in gastroenteropancreatic neuroendocrine neoplasia. Ann Clin Lab Sci 2019;49:448-456.

4   Ferrata M, Schad A, Zimmer S, Musholt TJ, Bahr K, Kuenzel J, Becker S, Springer E, Roth W, Weber MM, Fottner C: Pd-l1 expression and immune cell infiltration in gastroenteropancreatic (gep) and non-gep neuroendocrine neoplasms with high proliferative activity. Front Oncol 2019;9:343.

5   Sampedro-Nunez M, Serrano-Somavilla A, Adrados M, Cameselle-Teijeiro JM, Blanco-Carrera C, Cabezas-Agricola JM, Martinez-Hernandez R, Martin-Perez E, Munoz de Nova JL, Diaz JA, Garcia-Centeno R, Caneiro-Gomez J, Abdulkader I, Gonzalez-Amaro R, Marazuela M: Analysis of expression of the pd-1/pd-l1 immune checkpoint system and its prognostic impact in gastroenteropancreatic neuroendocrine tumors. Sci Rep 2018;8:17812.

6   Cives M, Strosberg J, Al Diffalha S, Coppola D: Analysis of the immune landscape of small bowel neuroendocrine tumors. Endocr Relat Cancer 2019;26:119-130.

7   Schultheis AM, Scheel AH, Ozretic L, George J, Thomas RK, Hagemann T, Zander T, Wolf J, Buettner R: Pd-l1 expression in small cell neuroendocrine carcinomas. Eur J Cancer 2015;51:421-426.

8   Capozzi M, C VONA, C DED, Ottaiano A, Tatangelo F, Romano GM, Tafuto S: Antiangiogenic therapy in pancreatic neuroendocrine tumors. Anticancer Res

18

2016;36:5025-5030.

9   Yu LL, Zhang YH, Zhao FX: Expression of indoleamine 2,3-dioxygenase in pregnant mice correlates with cd4+cd25+foxp3+ t regulatory cells. Eur Rev Med Pharmacol Sci 2017;21:1722-1728.

10   Ramjiawan RR, Griffioen AW, Duda DG: Anti-angiogenesis for cancer revisited: Is there a role for combinations with immunotherapy? Angiogenesis 2017;20:185-204.

11   Khan MS, Kirkwood A, Tsigani T, Garcia-Hernandez J, Hartley JA, Caplin ME, Meyer T: Circulating tumor cells as prognostic markers in neuroendocrine tumors. J Clin Oncol 2013;31:365-372.

12   Pinato DJ, Tan TM, Toussi ST, Ramachandran R, Martin N, Meeran K, Ngo N, Dina R, Sharma R: An expression signature of the angiogenic response in gastrointestinal neuroendocrine tumours: Correlation with tumour phenotype and survival outcomes. Br J Cancer 2014;110:115-122.

13   Velayoudom-Cephise FL, Duvillard P, Foucan L, Hadoux J, Chougnet CN, Leboulleux S, Malka D, Guigay J, Goere D, Debaere T, Caramella C, Schlumberger M, Planchard D, Elias D, Ducreux M, Scoazec JY, Baudin E: Are g3 enets neuroendocrine neoplasms heterogeneous? Endocr Relat Cancer 2013;20:649-657.

14   Marafioti T, Paterson JC, Ballabio E, Reichard KK, Tedoldi S, Hollowood K, Dictor M, Hansmann ML, Pileri SA, Dyer MJ, Sozzani S, Dikic I, Shaw AS, Petrella T, Stein H, Isaacson PG, Facchetti F, Mason DY: Novel markers of normal and neoplastic human plasmacytoid dendritic cells. Blood 2008;111:3778-3792.

15   Mazel M, Jacot W, Pantel K, Bartkowiak K, Topart D, Cayrefourcq L, Rossille D, Maudelonde T, Fest T, Alix-Panabieres C: Frequent expression of pd-l1 on circulating

19

breast cancer cells. Mol Oncol 2015;9:1773-1782.

16   Wang RF, Wang HY: Immune targets and neoantigens for cancer immunotherapy and precision medicine. Cell Res 2017;27:11-37.

17   Schalper KA, Carvajal-Hausdorf D, McLaughlin J, Altan M, Velcheti V, Gaule P, Sanmamed MF, Chen L, Herbst RS, Rimm DL: Differential expression and significance of pd-l1, ido-1 and b7-h4 in human lung cancer. Clin Cancer Res 2016

18   Khan KA, Kerbel RS: Improving immunotherapy outcomes with anti-angiogenic treatments and vice versa. Nat Rev Clin Oncol 2018;15:310-324.

19   da Silva A, Bowden M, Zhang S, Masugi Y, Thorner AR, Herbert ZT, Zhou CW, Brais L, Chan JA, Hodi FS, Rodig S, Ogino S, Kulke MH: Characterization of the neuroendocrine tumor immune microenvironment. Pancreas 2018;47:1123-1129.

20   Taube JM, Klein A, Brahmer JR, Xu H, Pan X, Kim JH, Chen L, Pardoll DM, Topalian SL, Anders RA: Association of pd-1, pd-1 ligands, and other features of the tumor immune microenvironment with response to anti-pd-1 therapy. Clin Cancer Res 2014;20:5064-5074.

21   Cassetta L, Kitamura T: Targeting tumor-associated macrophages as a potential strategy to enhance the response to immune checkpoint inhibitors. Front Cell Dev Biol 2018;6:38.

22   Pardoll DM: The blockade of immune checkpoints in cancer immunotherapy. Nat Rev Cancer 2012;12:252-264.

23   Wainwright DA, Dey M, Chang A, Lesniak MS: Targeting tregs in malignant brain cancer: Overcoming ido. Front Immunol 2013;4:116.

24   Zhai L, Ladomersky E, Lenzen A, Nguyen B, Patel R, Lauing KL, Wu M,

20

Wainwright DA: Ido1 in cancer: A gemini of immune checkpoints. Cell Mol Immunol 2018;15:447-457.

25   Johnson DB, Bordeaux J, Kim JY, Vaupel C, Rimm DL, Ho TH, Joseph RW, Daud AI, Conry RM, Gaughan EM, Hernandez-Aya LF, Dimou A, Funchain P, Smithy J, Witte JS, McKee SB, Ko J, Wrangle JM, Dabbas B, Tangri S, Lameh J, Hall J, Markowitz J, Balko JM, Dakappagari N: Quantitative spatial profiling of pd-1/pd-l1 interaction and hla-dr/ido-1 predicts improved outcomes of anti-pd-1 therapies in metastatic melanoma. Clin Cancer Res 2018;24:5250-5260.

26   Long GV, Dummer R, Hamid O, Gajewski TF, Caglevic C, Dalle S, Arance A, Carlino MS, Grob JJ, Kim TM, Demidov L, Robert C, Larkin J, Anderson JR, Maleski J, Jones M, Diede SJ, Mitchell TC: Epacadostat plus pembrolizumab versus placebo plus pembrolizumab in patients with unresectable or metastatic melanoma (echo-301/keynote-252): A phase 3, randomised, double-blind study. Lancet Oncol 2019;20:1083-1097.

27   Ricciuti B, Leonardi GC, Puccetti P, Fallarino F, Bianconi V, Sahebkar A, Baglivo S, Chiari R, Pirro M: Targeting indoleamine-2,3-dioxygenase in cancer: Scientific rationale and clinical evidence. Pharmacol Ther 2019;196:105-116.

28   Bosch F, Bruwer K, Altendorf-Hofmann A, Auernhammer CJ, Spitzweg C, Westphalen CB, Boeck S, Schubert-Fritschle G, Werner J, Heinemann V, Kirchner T, Angele M, Knosel T: Immune checkpoint markers in gastroenteropancreatic neuroendocrine neoplasia. Endocr Relat Cancer 2019;26:293-301.

29   Lamarca A, Nonaka D, Breitwieser W, Ashton G, Barriuso J, McNamara MG, Moghadam S, Rogan J, Mansoor W, Hubner RA, Clark C, Chakrabarty B, Valle JW: Pd-

21

l1 expression and presence of tils in small intestinal neuroendocrine tumours. Oncotarget 2018;9:14922-14938.

30   Pinato DJ, Black JR, Trousil S, Dina RE, Trivedi P, Mauri FA, Sharma R: Programmed cell death ligands expression in phaeochromocytomas and paragangliomas: Relationship with the hypoxic response, immune evasion and malignant behavior. Oncoimmunology 2017;6:e1358332.

31   Wiedenmann B, Pavel M, Kos-Kudla B: From targets to treatments: A review of molecular targets in pancreatic neuroendocrine tumors. Neuroendocrinology 2011;94:177-190.

32   Khan MS, Kirkwood AA, Tsigani T, Lowe H, Goldstein R, Hartley JA, Caplin ME, Meyer T: Early changes in circulating tumor cells are associated with response and survival following treatment of metastatic neuroendocrine neoplasms. Clin Cancer Res 2016;22:79-85.

33   Wang X, Sun Q, Liu Q, Wang C, Yao R, Wang Y: Ctc immune escape mediated by pd-l1. Med Hypotheses 2016;93:138-139.

34   Satelli A, Batth IS, Brownlee Z, Rojas C, Meng QH, Kopetz S, Li S: Potential role of nuclear pd-l1 expression in cell-surface vimentin positive circulating tumor cells as a prognostic marker in cancer patients. Sci Rep 2016;6:28910.

22

Figure Legends.

Figure 1. Panels A-C. Representative sections demonstrating PD-L1, PD-L2 and IDO-1 expression in NETs. **Panels D-E.** The distribution of PD-L1 and PD-L2 immunopositivity across site of origin and tumour grade, illustrating enrichment of PD-L1 expression in lung NETs and PD-L2 expression in pancreatic NETs. **Panels F-G** illustrate the relationship between PD-ligands expression and the presence of tumour necrosis or vascular invasion.

Figure 2. Panels A-B. Representative sections of a PD-L1-expressing NET (**Panel A**) co-immunostained for CD8 (red chromogen), CD4 (brown chromogen), PD-1 (blue chromogen) and FOXP3 (green chromogen) using multiplex immunohistochemistry. These illustrate enrichment of a CD8$^+$/PD-1$^+$ and CD4$^+$/FOXP3$^+$ immune-suppressive infiltrate in PD-L1-expressing NETs (**Panels C-D**). **Panel E.** Histogram illustrating the inverse relationship between CD8$^+$/PD-1$^+$ and CD4$^+$/FOXP3$^+$ tumour infiltrating lymphocytes (TILs) density and tumour grade. **Panels F-G**. Histograms illustrating the relationship between CD4, CD8 (**Panel F**) and CD8$^+$/PD-1$^+$ and CD4$^+$/FOXP3$^+$ TILs in NETs (**Panel G**). **Panel H.** Histograms documenting the positive association between CD8$^+$/PD-1$^+$ and CD4$^+$/FOXP3$^+$ TILs and tumour necrosis. **Panel I.** Illustrates the PD-L1

23

and PD-L2 immunolabelling of cyto-cell block samples of pNET immortalized cell lines QGP-1 and BON-1 in relationship to MDA-MB-231 breast cancer lines used as positive controls. **Panel L.** Immunoblot for PD-L1, Carbonic Anhydrase IX (CaIX) and beta-actin showing the independence of PD-L1 expression from hypoxia in QGP-1 and BON-1 immortalised cell lines following a 24-hours incubation in a 1% oxygen atmosphere (hypoxia, H) in comparison with normoxic (N) or untreated controls (C). MDA-MB-231 cells, where PD-L1 is strongly induced during hypoxia, were used as positive controls.

Figure 3. Panel A. Targeted transcriptomic analysis of G3WD-NETs (n=10) using Nanostring PanCancer Immune profiling illustrating the differential regulation of 22 gene expression signatures on the basis of site of origin (gastrointestinal, GI versus extra-gastrointestinal, eGI) and poor prognosis ($\leq$12 months vs >12 months OS). GI NETs display reduced expression of cancer-testis antigens (CT antigen) and lower expression of transcripts involved in immune-cell cytotoxicity compared to eGI NETs. **Panel B.** Volcano plot of differentially-regulated genes identified by Nanostring analysis. The Benjamini-Hockberg p-values are correlated to fold-changes in transcripts identified in G3WD-NETs with poor prognosis (defined as OS <12 months, n=6) versus G3WD-NETs with good prognosis (OS >12 months, n=4). Transcripts achieving statistical significance (FDR q-value of 5%) are highlighted by the presence of the corresponding gene name.

Figure 4. Panel A. Determination of PD-L1 expression in circulating tumour cells (CTCs) isolated from patients with NETs and in SKBR3 cells spiked into a healthy donor sample as a positive control. The specificity of PD-L1 immunostaining is proven by negative immunostaining with the isotypic control antibody and by positive staining in peripheral blood lymphocytes. **Panel B.** Proportion of PD-L1 immunopositive CTCs

24

across the sampled patients with NETs (n=12).

Table 1. General characteristics of the patient population.

Baseline characteristic	n=102, (%)
Gender	
Male	52 (51)
Female	50 (49)
Age, years	
<55	57 (56)
≥55	45 (44)
Primary site	
Pancreas	53 (52)
Midgut	18 (18)
Lung	30 (29)
Others	1 (1)
Tumour size, cm	
<3.0	69 (67)
≥3.0	33 (33)
Stage	
Limited disease	42 (43)
Loco regional lymphnodal spread	28 (27)
Metastatic disease	31 (30)
Functional status	
Non-functioning	69 (67)
Functioning	33 (33)
Insulinoma	21 (21)
Gastrinoma	9 (10)
Others	3 (3)
Tumour Necrosis	
Absent	76 (75)
Present	26 (25)
Angioinvasion	
Absent	67 (66)
Present	35 (34)
Grading (WHO Criteria 2010)	
G1-2	83 (82)
G3	19 (18)

Table 2. Preliminary evaluation of the relationship between patient characteristics, CTC counts and PD-L1 expression on CTCs.

Patient ID	Age	Primary	Metastases	OS (Months)	Status	WHO Grade	CTC Count	PD-L1(+) CTCs (%)
1	55	Gastric	Liver, lymphnodes	5.7	Dead	3	4	3 (75)
2	44	Small Bowel	Liver	25.4	Alive	2	2	1 (50)
3	45	Gastric	Liver, lymphnodes	8.8	Dead	3	1	1 (100)
4	65	Unknown	Bone, Lungs	29.1	Alive	1	4	4 (100)
5	61	Large Bowel	Liver, lymphnodes	1.9	Dead	2	4	4 (100)
6	54	Small Bowel	Liver	29.8	Alive	1	0	0
7	59	Gastric	Liver	18.4	Dead	2	1	0
8	74	Small Bowel	Liver, peritoneal	27.3	Alive	2	6	5 (83)
9	67	Pancreas	Liver	29.6	Alive	1	0	0
10	65	Pancreas	Liver	28.9	Alive	2	2	1 (50)
11	62	Pancreas	Liver	22.6	Dead	1	2	2 (100)
12	47	Pancreas	Liver	5.6	Dead	3	4	3 (75)

1

Figure 1.

Figure 2.

I.

	PD-L1	PD-L2
MDA-MB-231		
QGP-1		
BON-1		

L.

|	MDA-MB-231	QGP-1	BON-1	
	N H	C N H	C N H	
				CaIX
				PD-L1
				β-actin
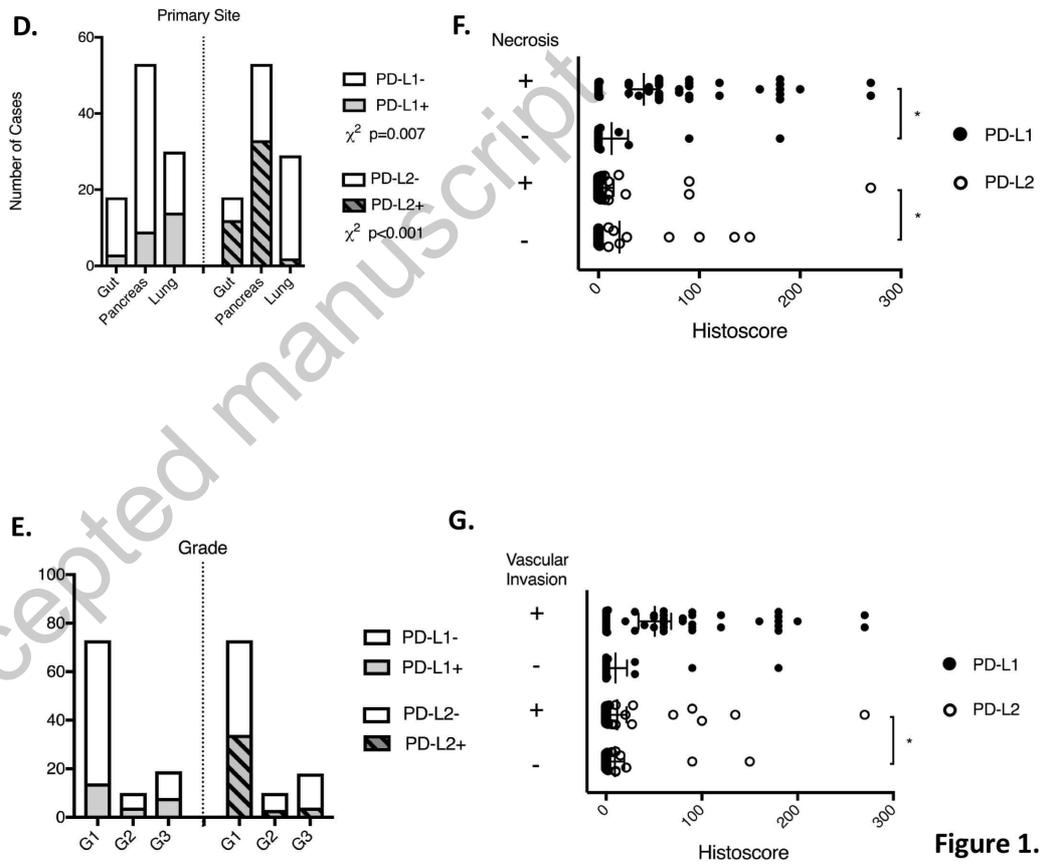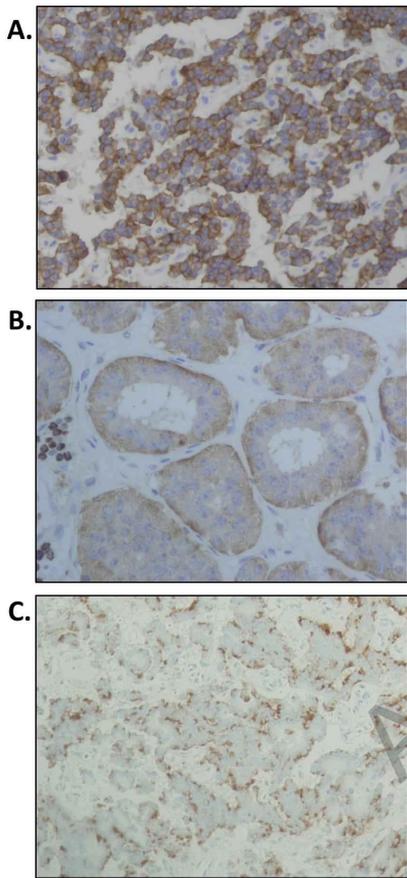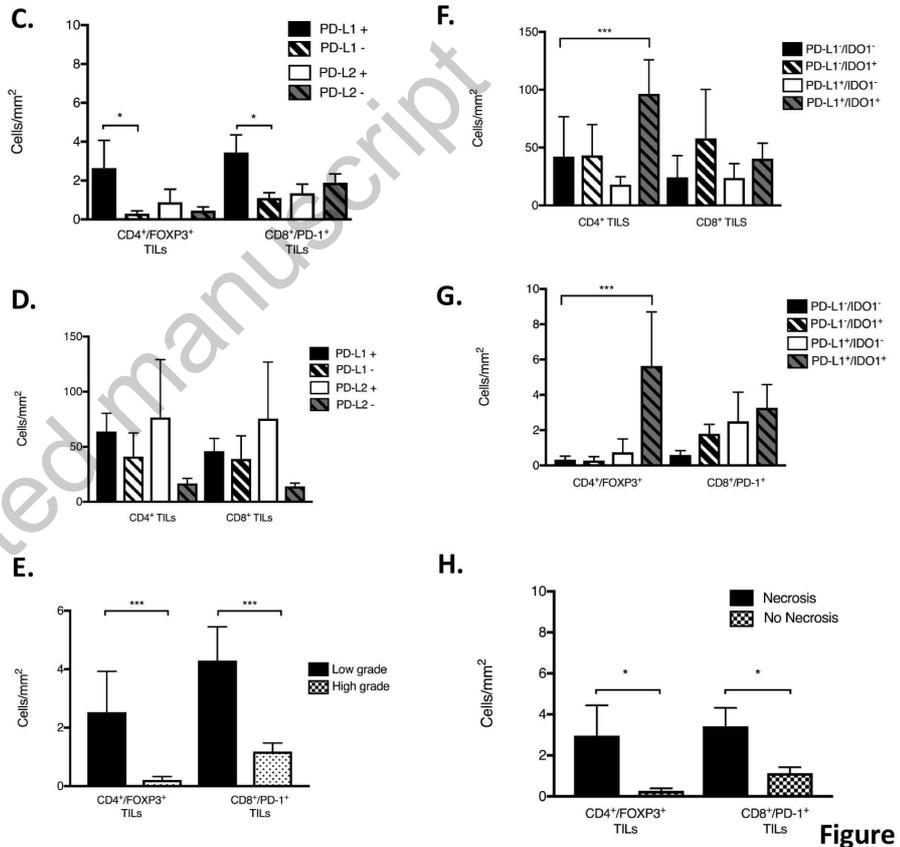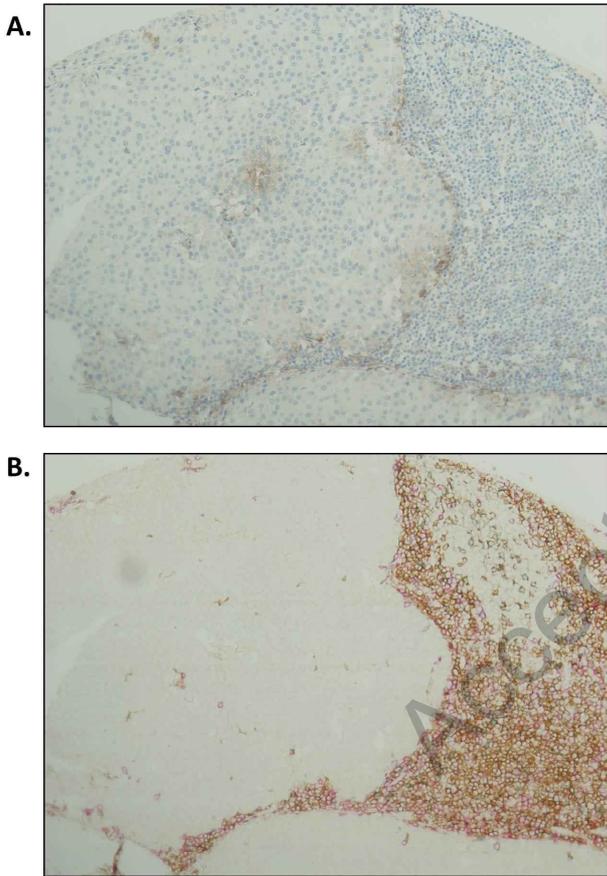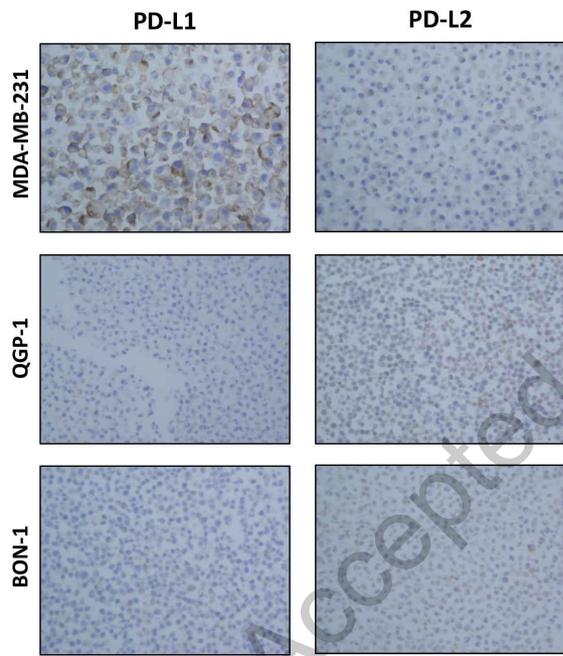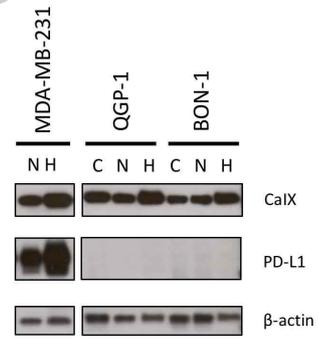
**Figure 2.**

A.
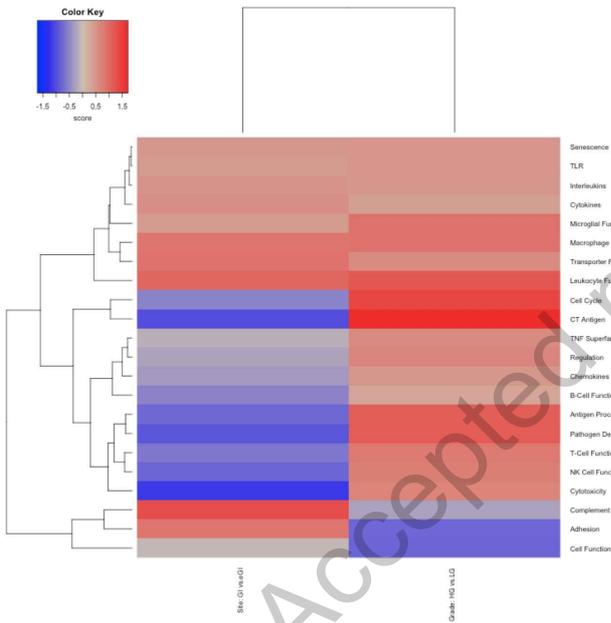
B.
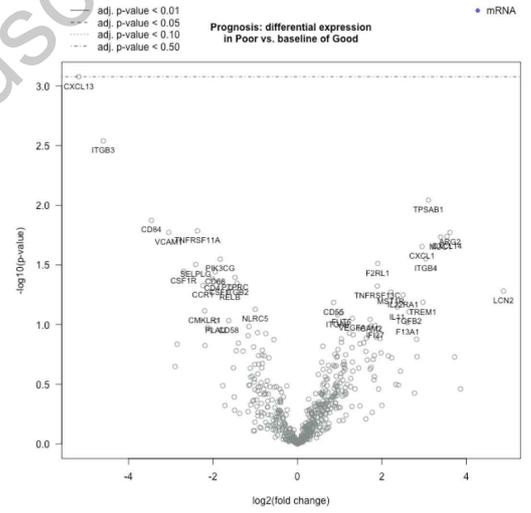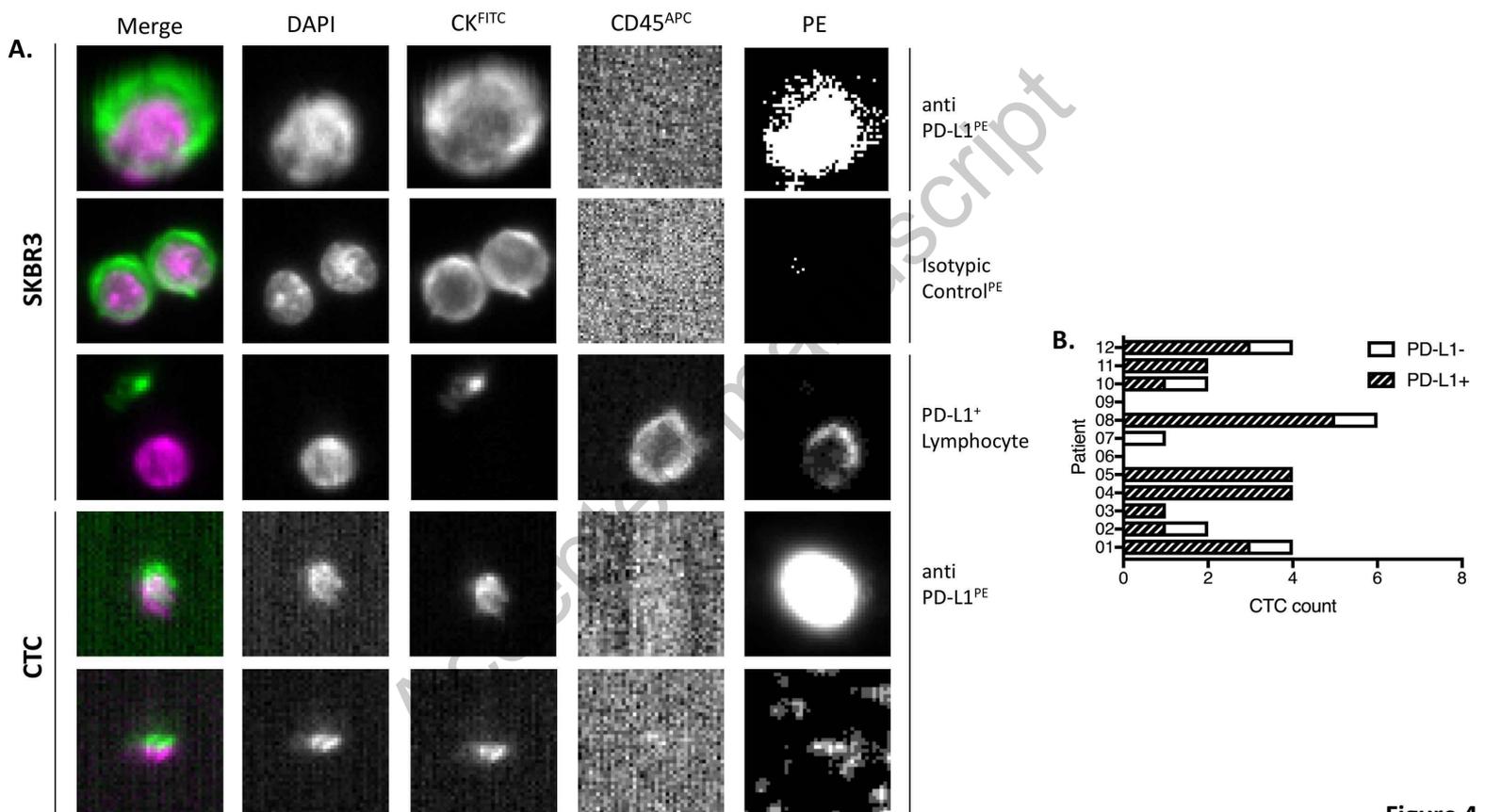
Figure 3.

Figure 4.

Supplementary Materials and Methods.

Programmed cell death ligands expression drives immune tolerogenesis across the diverse subtypes of neuroendocrine tumours.

David J. Pinato et al.

Cell Culture. BON-1 (RRID:CVCL_3985), QGP-1 (RRID:CVCL_3143), MDA-MB-231 (RRID:CVCL_0062) and SKBR3 (RRID:CVCL_0033) cell lines were purchased from the American Type Tissue Collection (ATCC). Cell lines were grown in either Dulbecco Modified Eagle's Medium or Roswell Park Memorial Institute Medium as recommended by ATCC guidance. Media were supplemented with 1% penicillin/streptomycin and 10% (v/v) fetal calf serum (Sigma Aldrich, St. Louis, MO, USA) and grown at 37 °C in 5% CO_2 atmosphere. Cells were routinely tested for Mycoplasma contamination and tested negative prior to any of the experiments reported. Experiments were conducted within 5 passages from thawing of the original master aliquot.

Histology. Archival formalin fixed, paraffin embedded materials were retrieved. The diagnosis of NET, the presence of intra-tumoural necrosis and vascular invasion was confirmed by an accredited endocrine pathologist (RD) on diagnostic haematoxylin and eosin (H&E) slides. Complete clinical and follow up information was retrieved by review of medical records. Overall (cancer-specific) survival (OS) was calculated from the time of diagnosis to the time of death or last follow up appointment.

Tissue microarray (TMA) construction. TMA blocks were prepared Following review and marking of diagnostic H&E slides, we used an MTA-1 Manual Tissue Microarrayer (Beecher Instruments, Prairie, Wisconsin, USA) to obtain triplicate 1 mm cores from separate areas of the tumor tissue. Adequate sampling of the target lesions was confirmed on a freshly cut H&E section from the recipient TMA block prior to immunohistochemical studies.

Immunohistochemistry. TMA block sectioning and immunohistochemical staining was performed at the Imperial College Histopathology Laboratory (Hammersmith Hospital, London) using the Leica Bond RX stainer (Leica, Buffalo, Illinois, USA). Tissues were sectioned at 5 microns, de-paraffinized in xylene and rehydrated in graded alcohol solutions. Optimal heat-mediated antigen retrieval conditions and primary antibody dilutions were optimized on de-identified human tissues obtained from the diagnostic histopathology laboratory as indicated by the antibody manufacturer. In all cases, omission of the primary antibody on positive control tissue sections served as negative control reaction. Positive and negative controls were run with test samples in a single batch for each tested antibody. Antigen retrieval was carried out using a microwave oven at 900W according to standard operating procedures: briefly, the sections were de-paraffinized in xylene, rehydrated in graded alcohols and heated in a microwave oven at 900W for 20 min in citrate buffer at pH 6.0(16). Optimal antigen retrieval varied according to protein target and primary antibody: tissue slides were incubated in citrate buffer at pH 6.0 for 30 minutes prior to PD-L1 (Clone E1L3N; Cat. Nr. 13684 Cell Signaling Technology, Danvers, Massachusetts, USA) and IDO-1 (Clone D5J4E; Cat. Nr. 86630 Cell Signaling Technology) immunostaining and 20 minutes prior to PD-L2 (Cat. Nr. 3500395, Sigma Aldrich, St. Louis, Missouri, USA), VEGF-A (Santa Cruz Biotechnology, Santa Cruz, California, USA), Hif-1α (AbCam, Cambridge, UK) and Ki-67 (Leica Microsystems, Wetzlar, Germany). Tissue sections were incubated in pH 9.0 EDTA buffer for 30 minutes prior to CaIX (Novus Biologicals, Littleton, Colorado, USA) immunostaining. Before immunostaining, slides were cooled at room temperature and endogenous peroxidase activity was suppressed by incubation with a 3% solution of H_2O_2

3

for 5 minutes. Primary antibodies anti-PD-L1 were incubated overnight at the concentration 1:100 whereas anti-PD-L2 and anti-IDO antibodies were incubated overnight at the concentration 1:100 and 1:300 respectively. The primary antibody against Ki-67 was diluted to 1:800 whereas all the other antibodies were used at a 1:1000 dilution. Tissue sections were then incubated with the secondary antibody for 1 hour at room temperature and then processed using the Polymer-HRP Kit (BioGenex, San Ramon California, USA) with development in Diaminobenzidine and Mayer's Haematoxylin counterstaining.

Biomarker Scoring. Expression of the candidate biomarkers was evaluated taking into account the percentage of cells staining positively (0-100%) and the intensity of the signal (1-3) to derive a semi-quantitative histoscore (range 0-300) as described before(11). Every core was assessed individually and the mean of the three readings was calculated per every single case. Due to the focal nature of PD-L1 expression, specimens displaying at least moderate intensity and >1% proportion of PD-L1 staining of tumor were considered positive(13). To ensure reproducibility of the scoring system, two observers (FAM, DJP) scored all the cases independently and results were found to be consistent.

Immunoblot. The following primary antibodies were used: PD-L1 (E1L3N, Cell Signaling Technology Inc., Danvers, MA, USA); Carbonic Anhydrase (Novus Biologicals, Littleton Colorado), β-actin (AbCam, Cambridge, UK) and incubated overnight at the concentration of 1:1000. Following culture in standard or hypoxic conditions for 24h cells were washed in phosphate buffered saline solution (PBS) and lysed in RIPA buffer (Invitrogen, Paisley, UK) supplemented with phosphatase and protease inhibitor solution (Sigma, St. Louis, MO, USA). Following acrylamide gel electrophoresis and transfer to a polyvinyl-alcohol

membrane(14), protein lysates were probed with appropriately diluted primary antibodies

Cyto-cell block. BON-1, QGP-1 and MDA-MB-231 cell lines at the concentration of 1 x 10^7 were harvested from culture once 60-80% confluent, washed twice in phosphate buffered saline (PBS) and centrifuged at 600 rpm for 30 minutes. The pellet obtained after centrifugation was transferred to absorbent paper, placed in a histological cassette and fixed in formaldehyde solution 10% for 24 hours as described by Cristo et al.[1]. Two micron thick histological sections were evaluated for PD-L1 and PD-L2 expression by immunohistochemistry as described in Material and Methods.

Nanostring Immune Profiling. We performed targeted transcriptomic profiling using the NanoString PanCancer Immune panel on an nCounter® Analysis System (NanoString Technologies, Seattle, USA). Hybridization reactions were performed according to the manufacturer's instructions. The PanCancer Immune CodeSet (NanoString Technologies) contains a biotinylated capture probe for 770 target genes and 40 housekeeping genes. For each sample 200 ng of total RNA were hybridised to multi-colour-tagged reporter probes for 18 hours at 65°C and processed on an automated nCounter® Prep Station. Following purification and immobilisation of hybridized samples, target mRNA quantification was performed on an nCounter® Digital Analyzer, counting 600 fields of view per reaction. Quantified expression data were analyzed using the nSolver analysis software version 4.0. The resulting counts were normalized to the average counts for all control spikes in each sample and subsequently normalized using the geometric mean of the housekeeping genes.

CTC enumeration and PD-L1 staining. For CTC enumeration and evaluation of PD-L1 expression we utilized pre-published methodology developed within Prof. Alix Panabières' laboratory, described in Mazel et al[2]. Prior to patient sample analysis we confirmed the sensitivity and specificity of the protocol. As a positive control, we utilized a 7.5 ml EDTA-anticoagulated blood sample derived from a healthy volunteer where 200 SKBR3 immortalized breast cancer cells were inoculated prior to analysis. This confirmed a recovery rate of 82%, in line with previous studies. We confirmed detection PD-L1 staining in SKBR3 cells which was not replicated when the isotypic control was added to the reaction (Mouse IgG1 PE, Cat. N. IC002P, R&D Systems).

Supplementary References.

1.   Cristo AP, Goldstein HF, Faccin CS, Maia AL, Graudenz MS. Increasing diagnostic effectiveness of thyroid nodule evaluation by implementation of cell block preparation in routine US-FNA analysis. Arch Endocrinol Metab 2016; 60:367-73.

2.   Mazel M, Jacot W, Pantel K, Bartkowiak K, Topart D, Cayrefourcq L, et al. Frequent expression of PD-L1 on circulating breast cancer cells. Mol Oncol 2015; 9:1773-82.